ATLAS results on charmonium and B_c and exotic heavy hadrons

- J/ψ & $\psi(2S)$ at 13 TeV, ATLAS-CONF-2019-047
- $B_c^{\pm}/B^{\pm}$ at 8 TeV, arXiv:1912.02672 (subm. to PRD)
- P_c^{+} at 7-8 TeV, ATLAS-CONF-2019-048

Zijun Xu (SLAC)
on behalf of the ATLAS Collaboration
CHARM 2021, May 31 - June 4, Mexico

ATLAS Detector @LHC

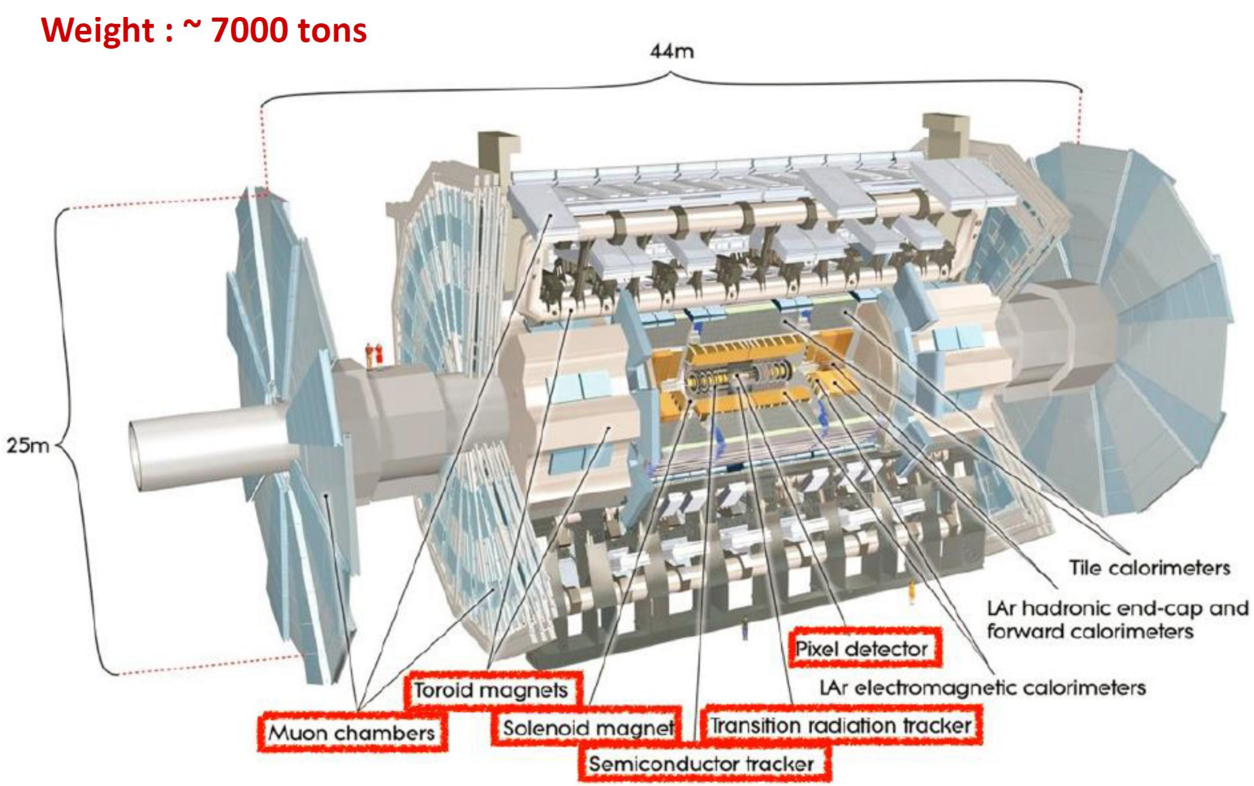

- Inner Detector (Pixel+SCT+TRT)
  - Pt>0.4(0.1) GeV, |η|<2.5
- Muon Spectrometer
  - Offline tracking: |η|<2.7
  - Triggering: |η|<2.4
- Run-2 improvements
  - Detector: IBL (Insertable B-layer), inner-most pixel layer(r=33mm) and thinner beam-pipe
    - resolution in mμμ: ~50 MeV at J/ψ mass, ~150 MeV at Y(nS) masses; ~10 μm impact parameter resolution
    - time resolution* ~60 fs after installation of IBL in Run 2 (30% improvement w.r.t. Run 1)
  - higher Luminosity and Sqrt(s) 7/8 TeV -> 13 TeV
  - Trigger upgrade to maintain low muon threshold at high lumi
- Great potential for new results in heavy flavor physics studies

ATLAS charmonium production

[ATL-COM-DAQ-2019-040]

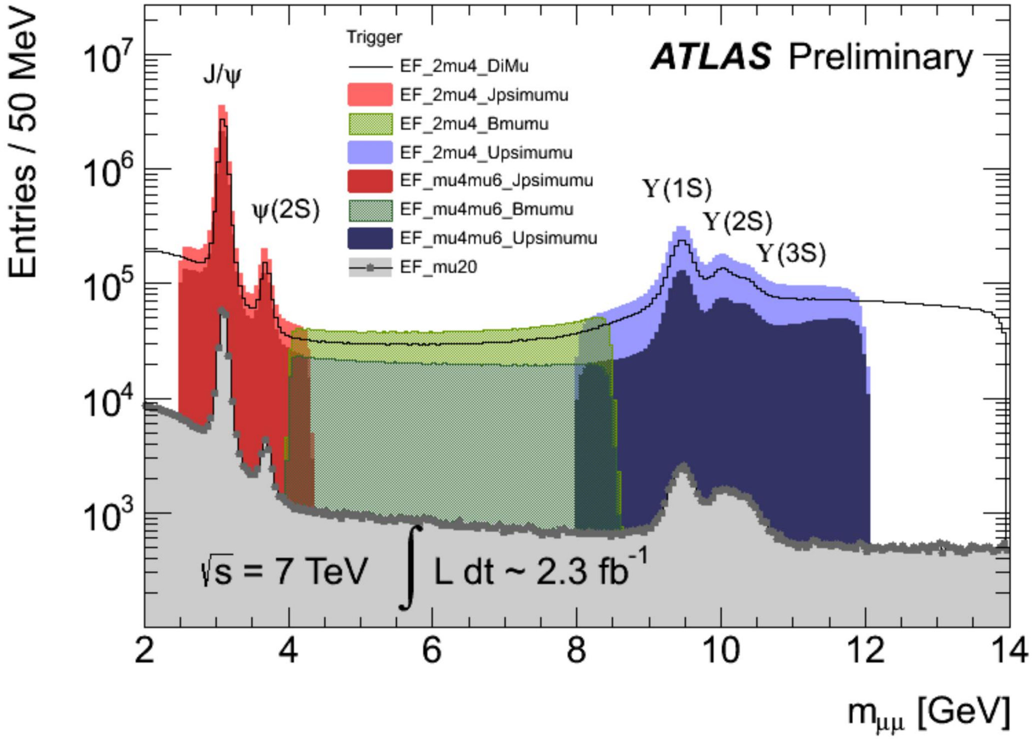

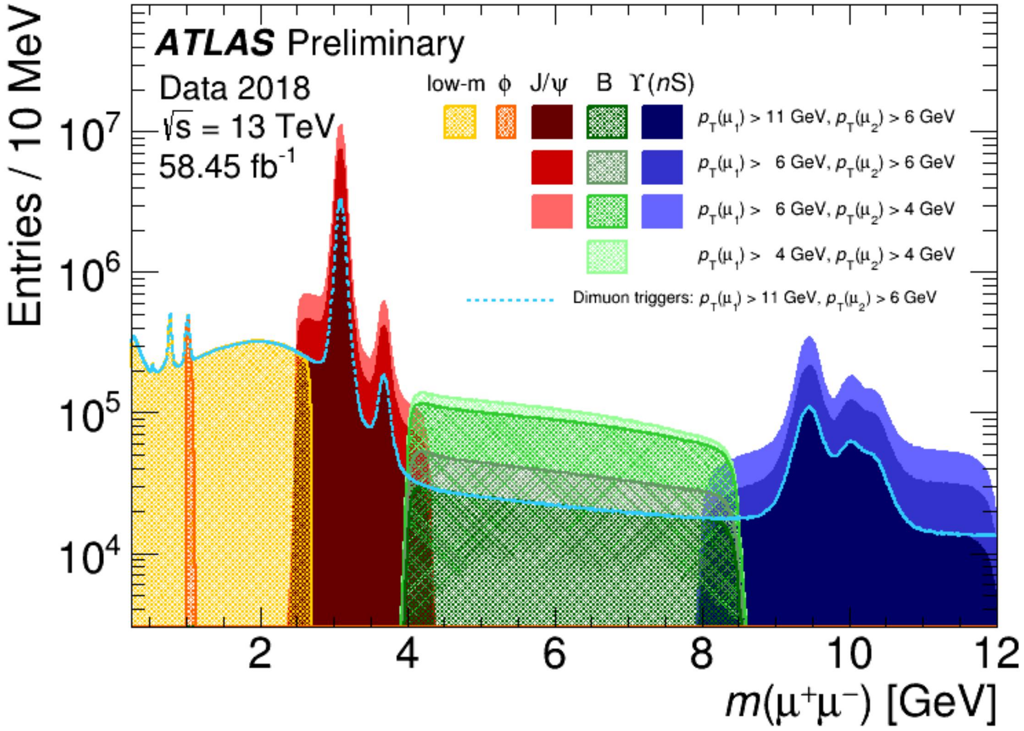

J/ψ and $\psi(2S)$ production

- studies of heavy quarkonia provide insight into QCD near boundary of perturbative and non-perturbative regimes
- cross section measurement is important for refining quarkonia production models
- ATLAS Run 1:
  - low-threshold dimuon triggers, limiting pT range to ~ 100 GeV
- ATLAS Run2
  - use single muon trigger with high threshold at 50 GeV , un-prescaled for the full Run2 data, 139 fb^{-1}
  - Provides coverage of the high-pT end of the distribution, well beyond previously achieved transverse momenta

J/ψ and ψ(2S): Mass and lifetime Fits

- pT 60-360 GeV for J/ψ in 11 bins (60-140 GeV for ψ(2S))
- Rapidity |y| < 2 covered in 3 bins
- Yields for J/ψ and ψ(2S), as well as both non-prompt fractions and ψ(2S) to J/ψ ratios determined from 2D fit
  - mass and pseudo-proper lifetime

$$\tau = \frac{m}{p_T}\frac{L_{xy}}{c}$$

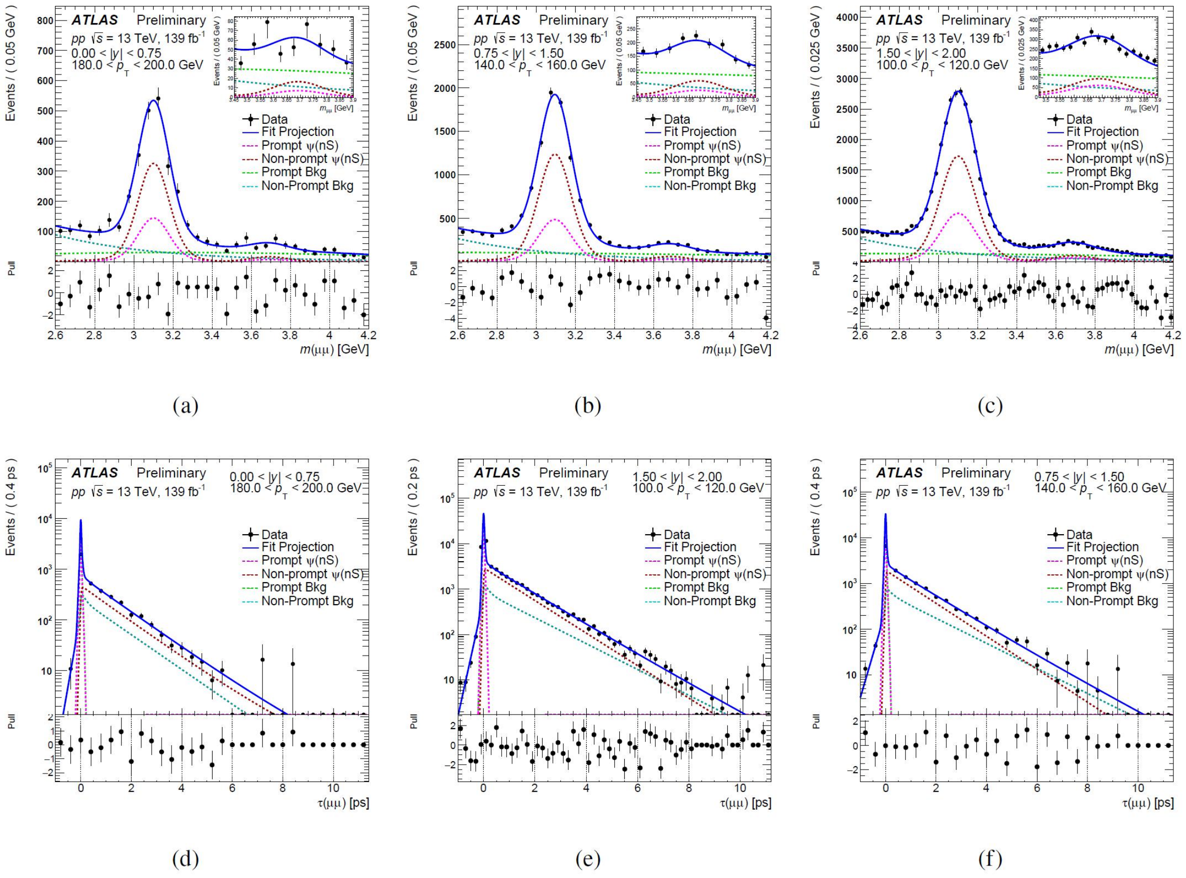

J/ψ and ψ(2S): non-prompt fractions

- Plateau at ~0.7 for pT >~ 40 GeV
- Similar behavior in pp and pp̄ collisions
- No strong dependence from rapidity
- Similar for J/ψ and ψ(2S)

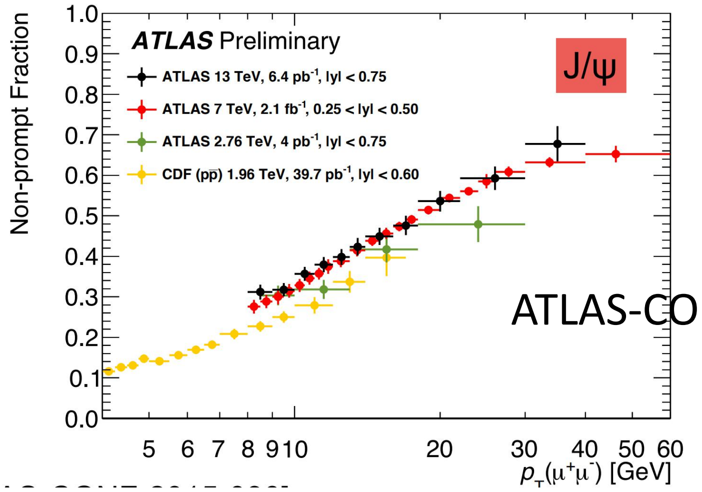

ATLAS-CONF-2015-030

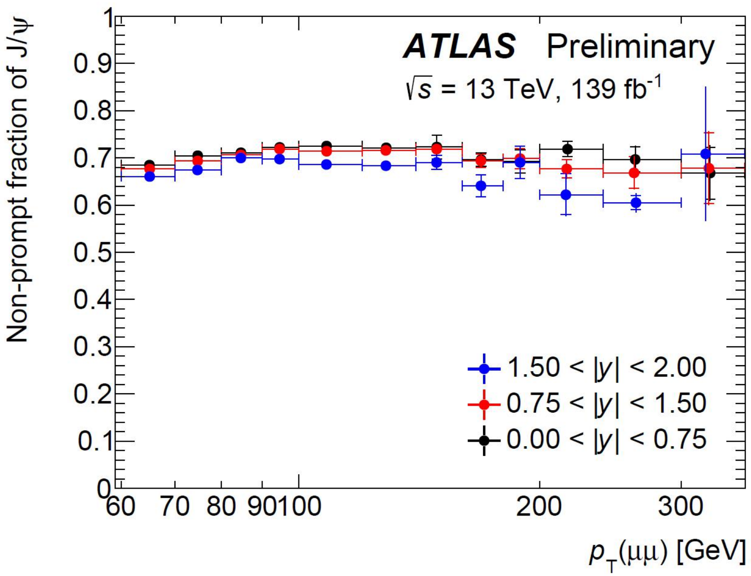

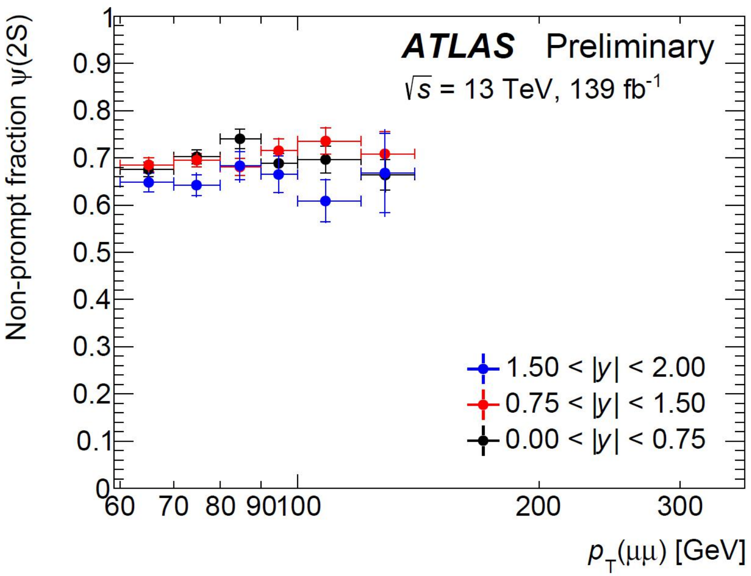

J/ψ and ψ(2S): non-prompt x-sections

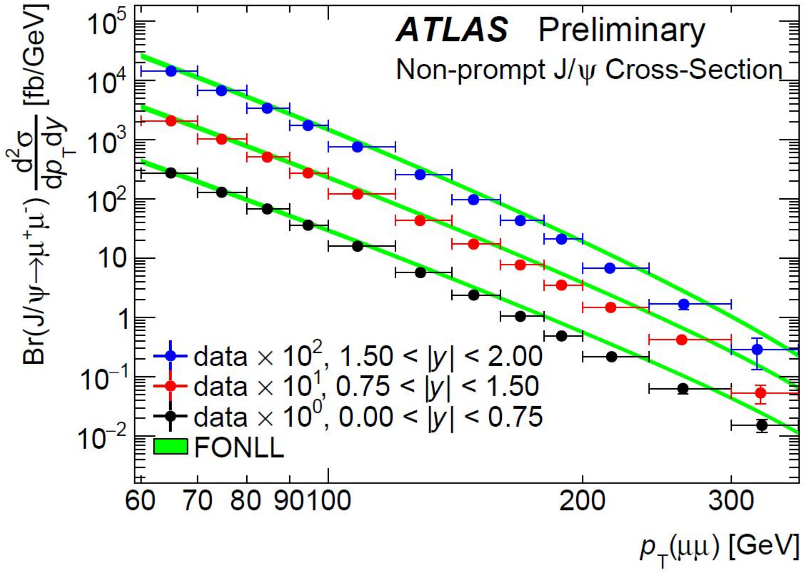

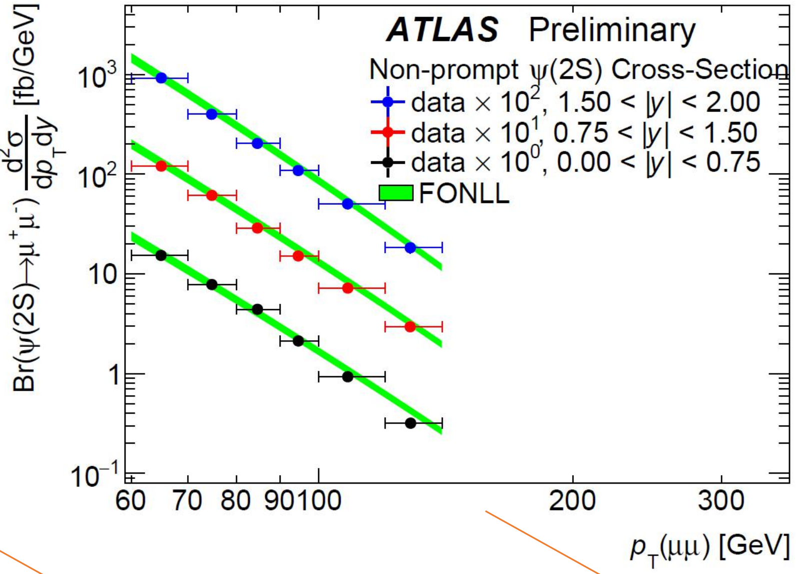

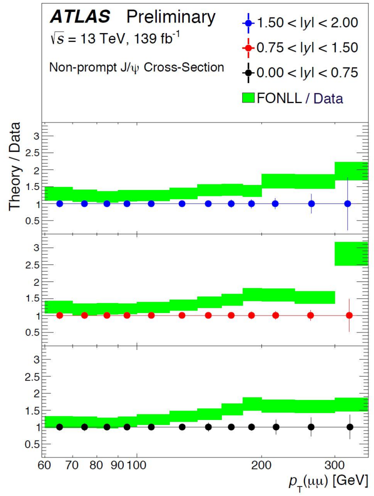

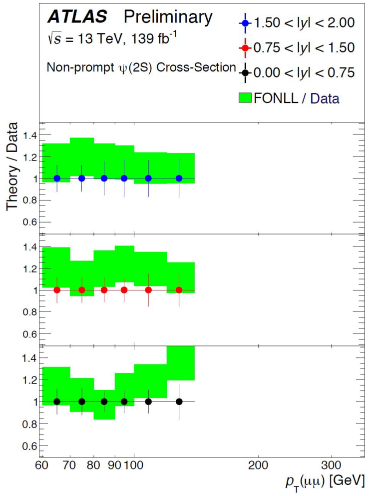

- FONLL predictions seem to work reasonably well over 5 orders of magnitude
  - http://www.lpthe.jussieu.fr/~cacciari/fonll/fonllform.html
- Deviation by a factor of 2 at hight-pT end

J/ψ: Prompt cross section at 13TeV

- ATLAS and CMS good agree in the overlap region
  - CMS, pT from 20 up to 120-150 GeV
    - PLB 780(2018) 251
  - Together smoothly cover 20-360 GeV
- Simple parameterisation describes data well, over 7 orders of magnitude
  - $(b+p_T)^{-n}$ with b=4.40, and n=5.91
- It would be interesting to see NRQCD predictions, especially for the high pT end

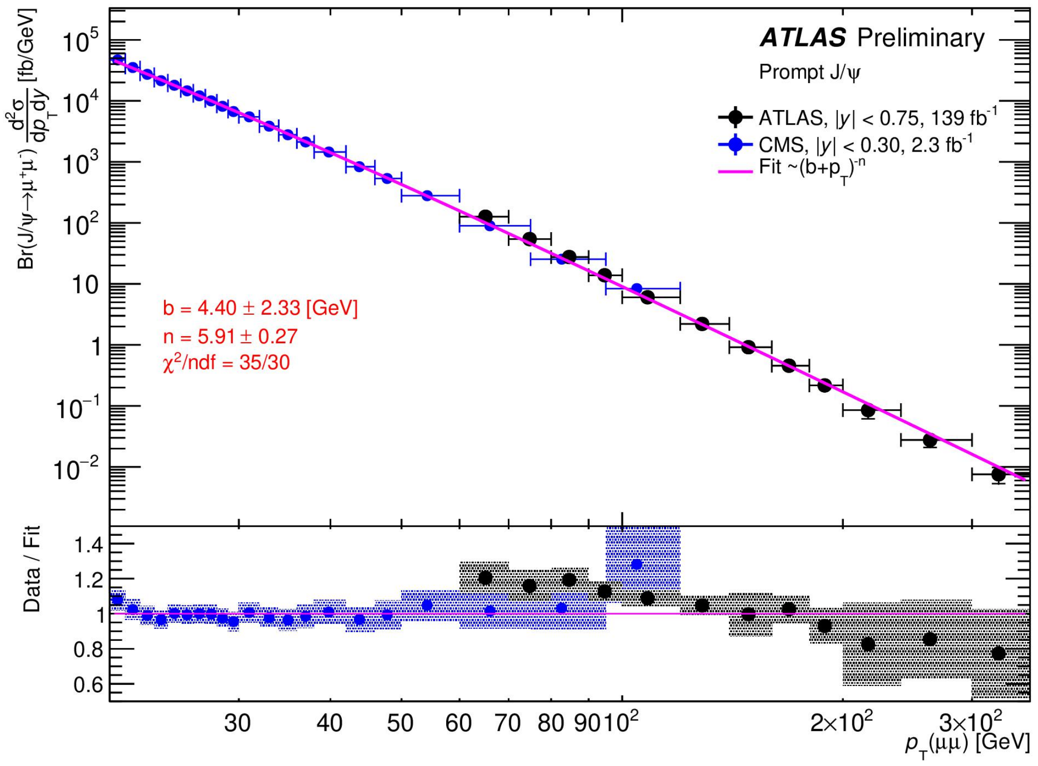

$B_c^\pm/B^\pm$ x-section ratios at 8TeV with 20fb^{-1}

- unique probe for heavy quark dynamics
  - $B_c^\pm$ is a bound state of two heaviest distinct quarks, b and c
- relative cross-section with similar decay mode for $B_c^\pm$ and $B^\pm$

$$\frac{\sigma(B_c^\pm)\cdot\mathcal{B}(B_c^\pm\to J/\psi\pi^\pm)\cdot\mathcal{B}(J/\psi\to\mu^+\mu^-)}{\sigma(B^\pm)\cdot\mathcal{B}(B^\pm\to J/\psi K^\pm)\cdot\mathcal{B}(J/\psi\to\mu^+\mu^-)}=\frac{N^{\text{reco}}(B_c^\pm)}{N^{\text{reco}}(B^\pm)}\cdot\frac{\epsilon(B^\pm)}{\epsilon(B_c^\pm)}.$$

- fiducial volume: pT >13 GeV, |y|<2.3
- 2 pT bin (13-22, >22 GeV), and 2 |y| bin (<0.75, 0.75-2.3)
- extended unbinned ML fits to the mass distributions of $B_c^\pm$ and $B^\pm$ to extract N^{reco} from the data in each bin

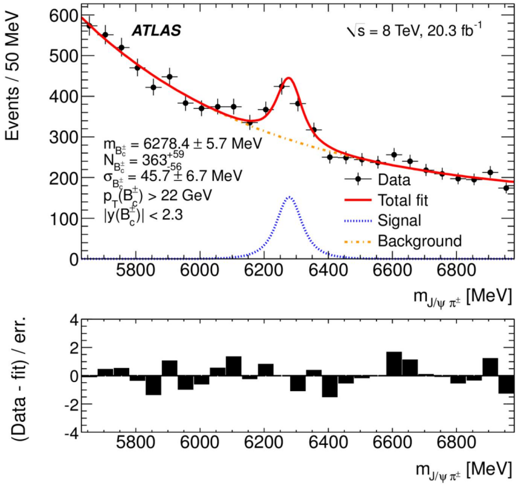

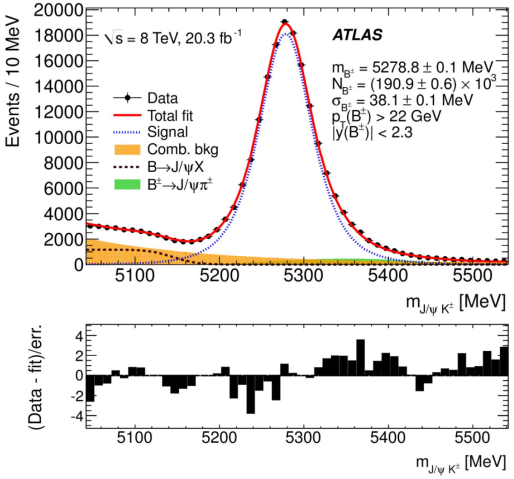

arXiv:1912.02672

$B_c^{\pm}/B^{\pm}$ x-section ratios

- relative X-section in fiducial region (horizontal line)

$$\frac{\sigma(B_c^{\pm})\cdot\mathcal{B}(B_c^{\pm}\to J/\psi\pi^{\pm})}{\sigma(B^{\pm})\cdot\mathcal{B}(B^{\pm}\to J/\psi K^{\pm})} = (0.34\ \pm\ 0.04_{\,\mathrm{stat}}\ {}^{+0.06}_{-0.02}{}_{\,\mathrm{syst}}\ \pm\ 0.01_{\mathrm{lifetime}})\%,$$

- 2 bins of pT and |y|:
  - ratio decreases with pT
  - no significant |y| dependency

- complements CMS and LHCb results

0.683 ± 0.018 ± 0.009	**pT < 20 GeV**, 2.0 < |y| < 4.5	LHCb at 8 TeV
0.48 ± 0.05 ± 0.03 ± 0.05	**pT > 15 GeV**, |y| < 1.6	CMS at 7 TeV
0.44 ± 0.07 $^{+0.09}_{-0.04}$ ± 0.01	**13 < pT** < 22 GeV, |y| < 2.3	ATLAS at 8 TeV
0.24 ± 0.04 $^{+0.05}_{-0.01}$ ± 0.01	**pT > 22 GeV**, |y| < 2.3	ATLAS at 8 TeV

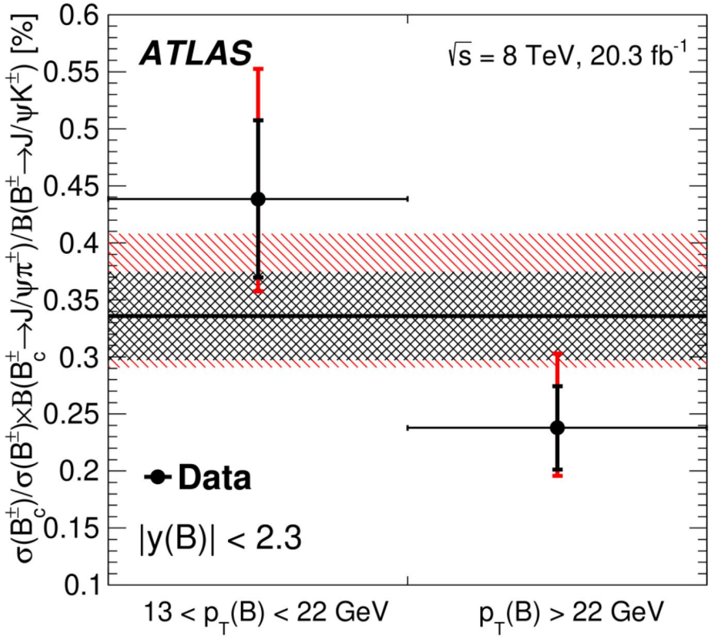

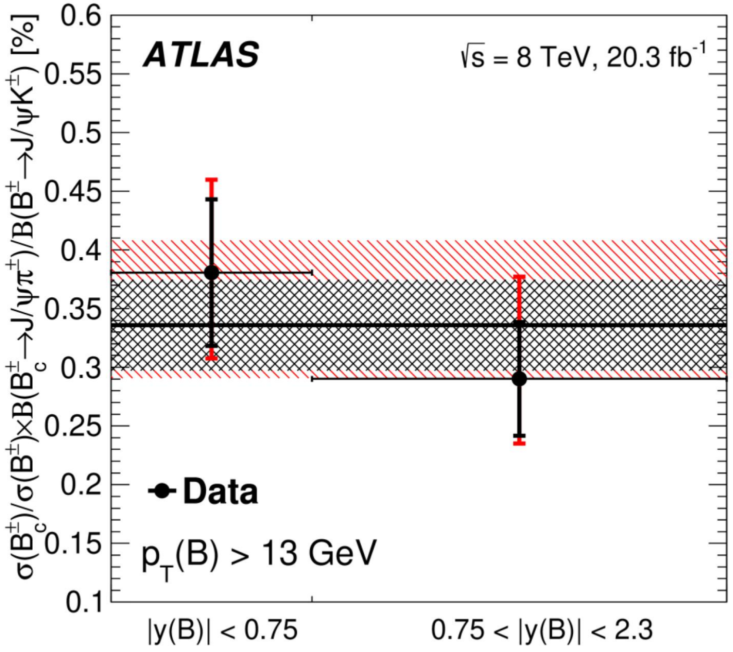

Pentaquark search in J/ψp

- LHCb: structures observed in J/ψp mass spectrum Λ^0_b->J/ψpK- decay
  - $P_c(4312)^+$, $P_c(4440)^+$ and $P_c(4457)^+$
  - hint for $P_c(4380)^+$

- not observed by GLUEX in γp->J/ψp s-channel
  - PRL 123 (2019) 072001

- D0: 3sigma unresolved $P_c(4440)$+$P_c(4457)$ peak in inclusive P_c->J/ψp channel
  - arXiv:1910.11767

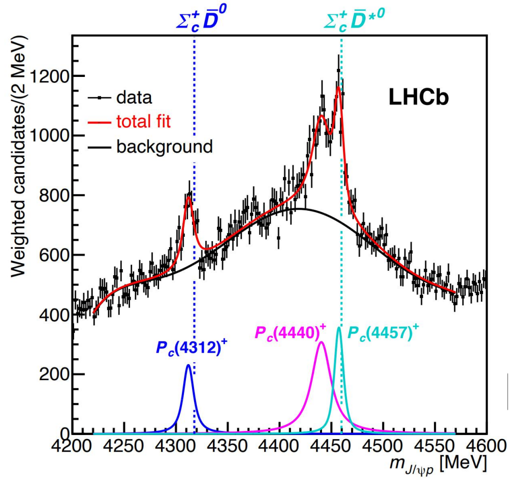

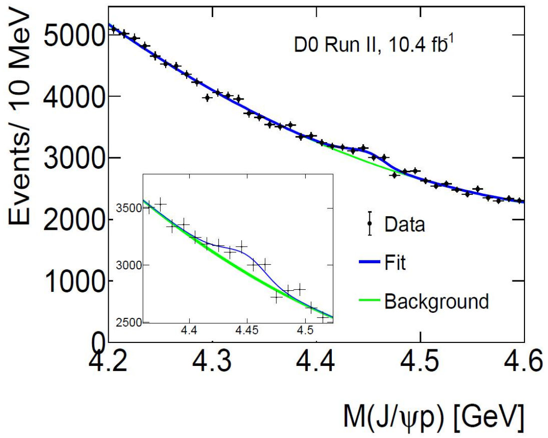

ATLAS-CONF-2019-048

ATLAS Pentaquark search in $\Lambda^0_b \to J/\psi p K^-$

- ATLAS search with $4.9 fb^{-1}$ (7TeV) and $20.9 fb^{-1}$ (8TeV) data
- no PID: No $\pi^\pm/K^\pm/p$ separation
  - need to consider all b hadrons decay to $J/\psi h_1 h_2$ candidates
- performing sequence of iterative fits in Λ^0_b signal region, $B^0(J/\psi \pi K)$ and $B^0_s(J/\psi KK)$ control regions and in full range of selected dataset
- $\Lambda^0_b \to J/\psi p K^-$ signal is observed on the top of
  - very large $B \to J/\psi K^+\pi^-$, large $Bs \to J/\psi K^+K^-$
  - large combinatorial background
  - tail from $B \to J/\psi \pi^+\pi^-$ and $Bs \to J/\psi \pi^+\pi^-$

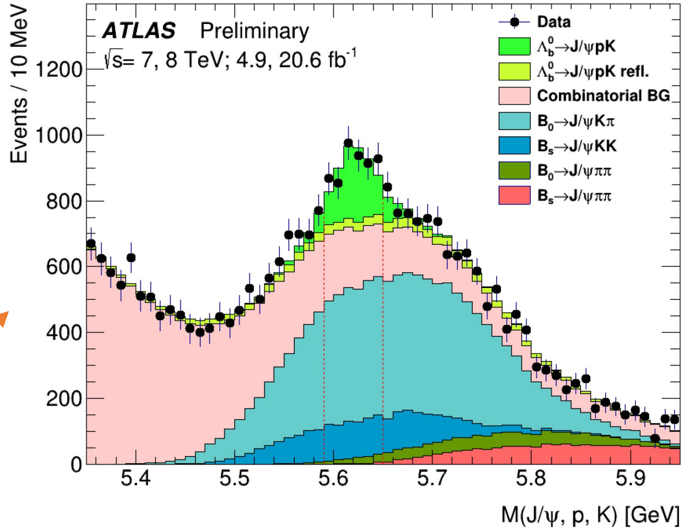

$N(\Lambda_b \to J/\psi,p,K) = 2270 \pm 300$

$N(B^0 \to J/\psi,K,\pi) = 10770$,
$N(B_s \to J/\psi,K,K) = 2290$,
$N(B^0 \to J/\psi,\pi,\pi) = 1070$,
$N(B_s \to J/\psi,\pi,\pi) = 1390$;

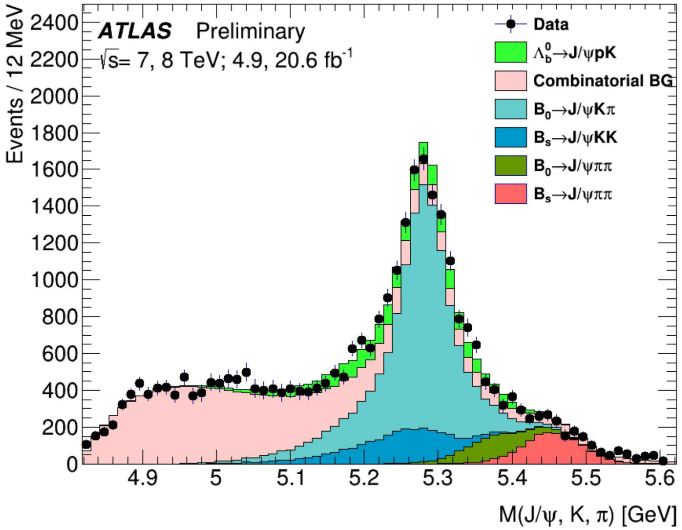

Fitting with 2 or 4 Pentaquarks

1010±140 direct $\Lambda_b \to J/\psi, p, K$

- Fitting with 2 pentaquarks hypothesis with spin parity of $3/2^-$ (light) and $5/2^+$(heavy)
  - good description of data: χ2/n.d.f = 37.1/39
  - systematic uncertainties comparable to statistical ones

Parameter	Value	LHCb value [5]
$N(P_{c1})$	$400^{+130}_{-140}(\text{stat})^{+110}_{-100}(\text{syst})$	–
$N(P_{c2})$	$150^{+170}_{-100}(\text{stat})^{+50}_{-90}(\text{syst})$	–
$N(P_{c1}+P_{c2})$	$540^{+80}_{-70}(\text{stat})^{+70}_{-80}(\text{syst})$	–
$\Delta\phi$	$2.8^{+1.0}_{-1.6}(\text{stat})^{+0.2}_{-0.1}(\text{syst})$ rad	–
$m(P_{c1})$	$4282^{+33}_{-26}(\text{stat})^{+28}_{-7}(\text{syst})$ MeV	4380 ± 8 ± 29 MeV
$\Gamma(P_{c1})$	140^{+77}_{-50} (stat)$^{+41}_{-33}$ (syst) MeV	205 ± 18 ± 86 MeV
$m(P_{c2})$	4449^{+20}_{-29} (stat)$^{+18}_{-10}$ (syst) MeV	4449.8 ± 1.7 ± 2.5 MeV
$\Gamma(P_{c2})$	51^{+59}_{-48} (stat)$^{+14}_{-46}$ (syst) MeV	39 ± 5 ± 19 MeV

- Fitting with 4 pentaquarks hypothesis
  - can NOT be distinguished because of low mass resolution
  - tested by fixing parameters to LHCb values
  - χ2/n.d.f = 37.1/42

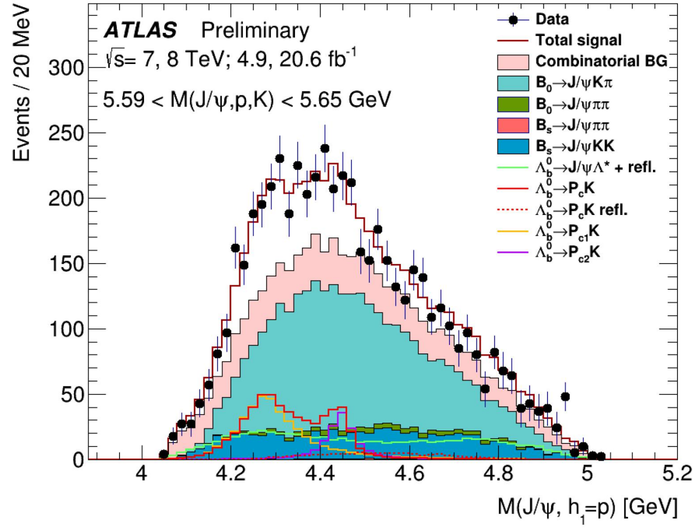

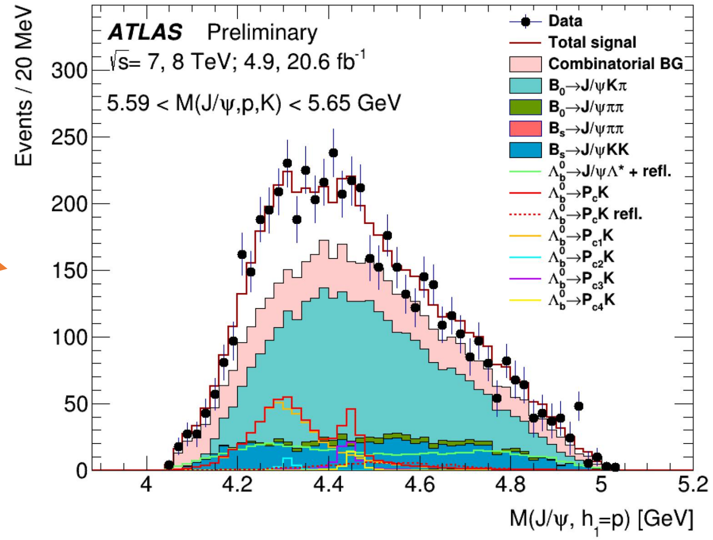

No-Pentaquark hypothesis

- $\chi 2$ fits of the mass distribution in the signal region for the hypothesis without pentaquarks with the extended $\Lambda^0_b \rightarrow J/\psi\Lambda^{*0}$ decay model
  - $\chi 2$/n.d.f = 42.0/23, p-value=9.1e-3

- Model without pentaquark disfavored but can't be excluded

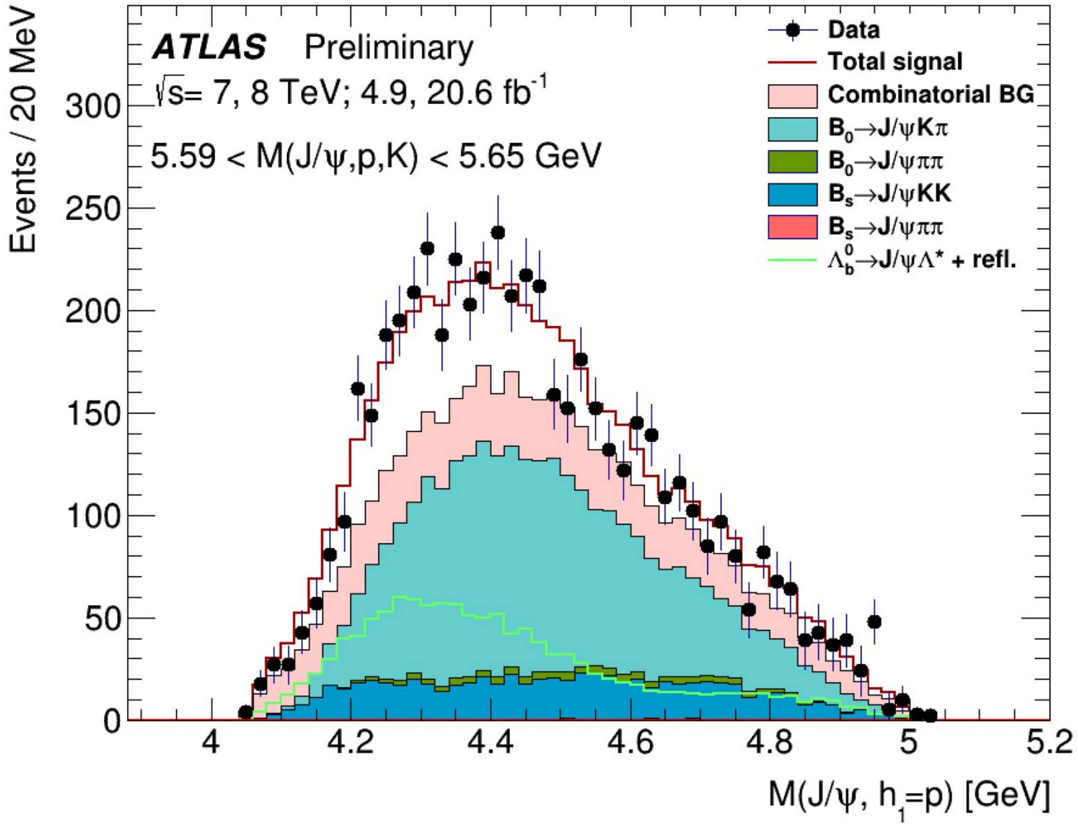

Summary

- ATLAS has a rich physics program for heavy flavor, selected results reported
  - J/ψ and $\psi(2S)$ production at high pT at 13TeV 139fb^{-1} data
    - non-prompt fraction ~0.7 for both J/ψ and $\psi(2S)$
    - non-prompt x-sec from FONLL tend to be higher than data at high pT end
  - $B^{\pm}_{c}/B^{\pm}$ production cross-section at 8TeV 20fb^{-1} data
    - complements LHCb and CMS measurements
    - the ratio decreases with pT, no significant |y| dependence
  - Pentaquark search at 7-8 TeV 25fb^{-1} data
    - Model with 2(or 4) pentaquarks Pc->$J/\psi p$ consistent with data (and with LHCb results)
    - no-pentaquark hypothesis disfavored but can’t be excluded so far
- stay tuned for the new results!

Backup

Data Taking

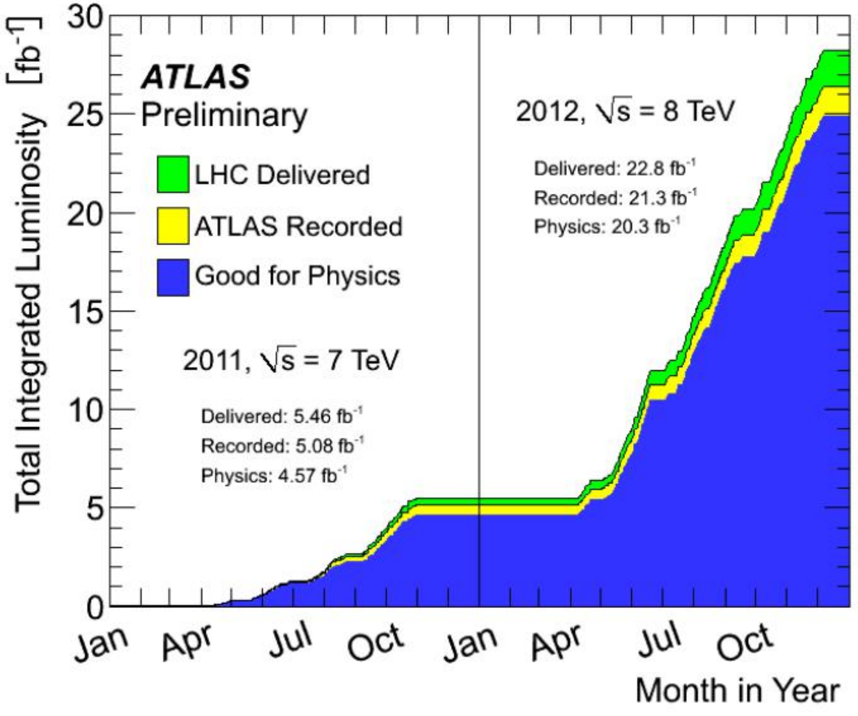

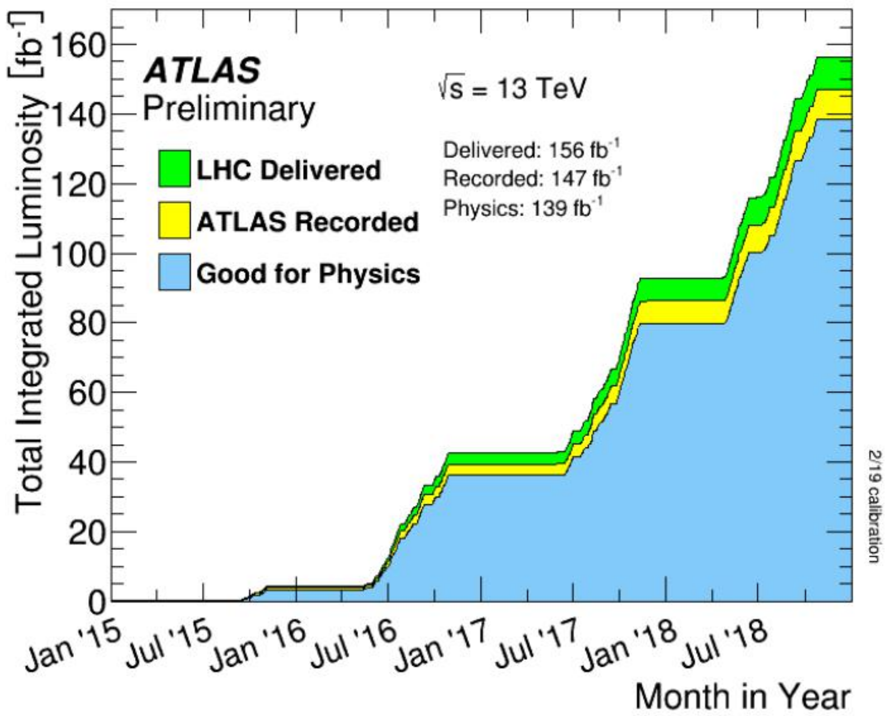

Peak Lumi: 7.73 x 10^{33} cm^{-2} s^{-1} **21.0 x 10^{33} cm^{-2} s^{-1}**

J/ψ and ψ(2S): Differential cross sections

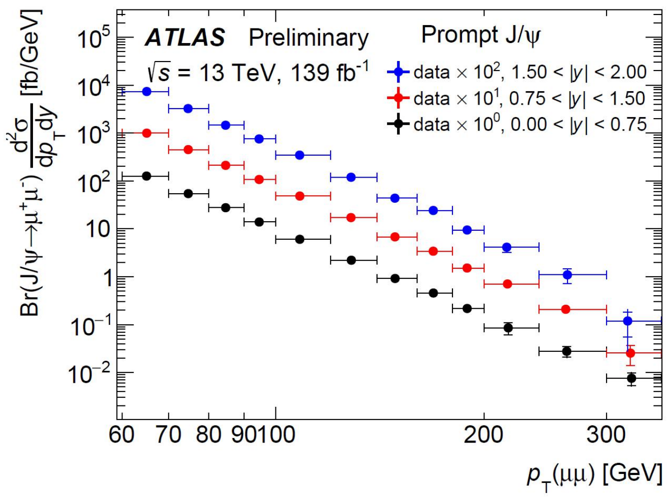

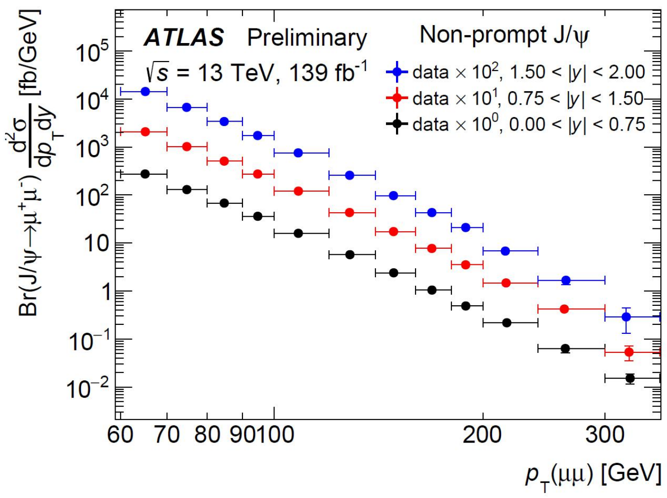

J/ψ

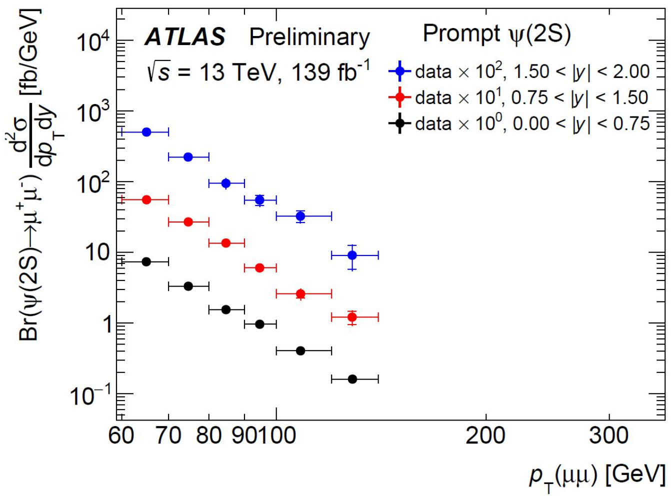

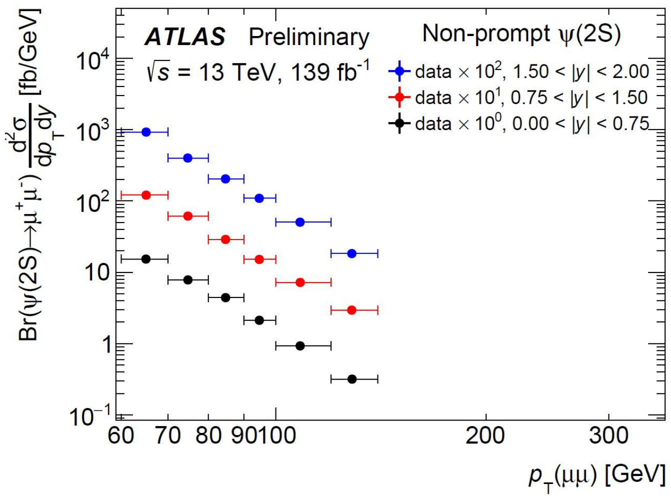

ψ(2s)

J/ψ and ψ(2S): fitting model

i	Type	P/NP	$f_i(m)$	$h_i(\tau)$
1	J/ψ	P	$\omega G_1(m) + (1-\omega)CB_1(m)$	$\delta(\tau)$
2	J/ψ	NP	$\omega G_1(m) + (1-\omega)CB_1(m)$	$E_1(\tau)$
3	$\psi(2S)$	P	$\omega G_2(m) + (1-\omega)CB_2(m)$	$\delta(\tau)$
4	$\psi(2S)$	NP	$\omega G_2(m) + (1-\omega)CB_2(m)$	$E_2(\tau)$
5	Bkg	P	B	$\delta(\tau)$
6	Bkg	NP	$E_4(m)$	$E_5(\tau)$
7	Bkg	NP	$E_6(m)$	$E_7(\|\tau\|)$

Notation	Function
G	Gaussian
CB	Crystal Ball
E	Exponential
B	Bernstein polynomials

Table 1: Parameterisation of the fit model. Notation is explained in the text and in the table on the right. Correlation between m and τ is introduced in one of the sub-terms for $i = 1$, see the text for details.

J/ψ and ψ(2S): uncertainties

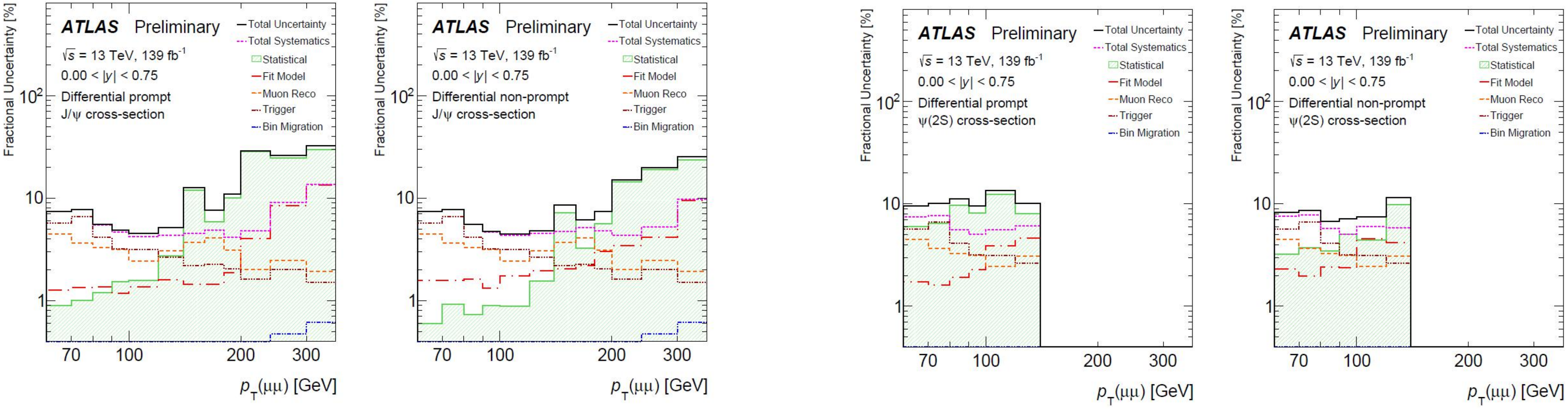

(a) (b) (c) (d)

Figure 2: The total, statistical, and systematic fractional uncertainties are shown as a function of p_T for (a) prompt J/ψ, (b) non-prompt J/ψ, (c) prompt $\psi(2S)$, (d) non-prompt $\psi(2S)$ mesons for the rapidity slice $|y| < 0.75$. The main components of the systematic uncertainties are also shown.

$B_c^{\pm}/B^{\pm}$ x-section ratios: yields

Table 1: Summary of the main parameters of the $B^{\pm}$ fits. The uncertainties quoted are statistical.

Analysis bin	Fitted mass of the $B^{\pm}$ [MeV]	Number of the $B^{\pm}$ candidates	σ_m of the $B^{\pm}$ [MeV]
$p_T(B) > 13$ GeV, $\lvert y(B)\rvert < 2.3$	5278.6 ± 0.1	$(398.3 \pm 0.8) \times 10^3$	37.5 ± 0.1
$13 < p_T(B) < 22$ GeV, $\lvert y(B)\rvert < 2.3$	5278.5 ± 0.1	$(207.6 \pm 0.6) \times 10^3$	37.5 ± 0.1
$p_T(B) > 22$ GeV, $\lvert y(B)\rvert < 2.3$	5278.8 ± 0.1	$(190.9 \pm 0.6) \times 10^3$	38.1 ± 0.1
$p_T(B) > 13$ GeV, $\lvert y(B)\rvert < 0.75$	5278.4 ± 0.1	$(147.9 \pm 0.5) \times 10^3$	26.6 ± 0.1
$p_T(B) > 13$ GeV, $0.75 < \lvert y(B)\rvert < 2.3$	5279.1 ± 0.1	$(248.8 \pm 0.6) \times 10^3$	45.9 ± 0.1

Table 2: Summary of the main parameters of the $B_c^{\pm}$ fits. The uncertainties quoted are statistical.

Analysis bin	Fitted mass of the $B_c^{\pm}$ [MeV]	Number of the $B_c^{\pm}$ candidates	σ_m of the $B_c^{\pm}$ [MeV]
$p_T(B) > 13$ GeV, $\lvert y(B)\rvert < 2.3$	6281.0 ± 4.5	798^{+92}_{-84}	52.4 ± 5.6
$13 < p_T(B) < 22$ GeV, $\lvert y(B)\rvert < 2.3$	6283.7 ± 6.9	417^{+68}_{-63}	59.5 ± 9.2
$p_T(B) > 22$ GeV, $\lvert y(B)\rvert < 2.3$	6278.4 ± 5.7	363^{+59}_{-56}	45.7 ± 6.7
$p_T(B) > 13$ GeV, $\lvert y(B)\rvert < 0.75$	6275.1 ± 1.7	319^{+57}_{-52}	31.5 ± 5.7
$p_T(B) > 13$ GeV, $0.75 < \lvert y(B)\rvert < 2.3$	6275.2 ± 9.0	454^{+71}_{-66}	67.1 ± 10.4

arXiv:1912.02672

$B_c^{\pm}/B^{\pm}$ x-section ratios: uncertainties

Table 4: Summary of the absolute values of systematic uncertainties for the analysis efficiency ratios.

Source of uncertainty	Absolute value of the uncertainty in the efficiency ratio				
	$p_T > 13$ GeV	$13 < p_T < 22$ GeV	$p_T > 22$ GeV	$\lvert y\rvert < 0.75$	$0.75 < \lvert y\rvert < 2.3$
Size of the MC samples and the event counting	0.03	0.05	0.03	0.05	0.04
sPlot-based MC reweighting procedure	0.04	0.03	0.03	0.05	0.06
Minimal selection criteria	0.04	0.09	0.02	0.06	0.03
Tracking uncertainty	0.01	0.01	0.01	0.01	0.01

Table 5: Summary of all systematic uncertainties for the number of signal events in the two p_T bins.

Source of uncertainty	Uncertainty value			
	$B_c^{\pm}$		$B^{\pm}$	
	13 GeV $< p_T <$ 22 GeV	$p_T >$ 22 GeV	13 GeV $< p_T <$ 22 GeV	$p_T >$ 22 GeV
Signal model of the fit	2.4%	1.1%	0.1%	0.2%
CS and PRD components	$^{+19.3\%}_{-2.4\%}$	$^{+19.9\%}_{-2.4\%}$	0.5%	0.5%
Background model of the fit	1.7%	1.2%	0.2%	0.2%
Trigger and reconstruction effects	0.9%	0.8%	1.2%	1.2%
B-meson lifetime uncertainty	1.1%	0.9%	< 0.1%	< 0.1%

Table 6: Summary of all systematic uncertainties for the number of signal events in the two $|y|$ bins.

Source of uncertainty	Uncertainty value			
	$B_c^{\pm}$		$B^{\pm}$	
	$\lvert y\rvert < 0.75$	$0.75 < \lvert y\rvert < 2.3$	$\lvert y\rvert < 0.75$	$0.75 < \lvert y\rvert < 2.3$
Signal model of the fit	2.5%	2.8%	0.1%	0.2%
CS and PRD components	$^{+11.2\%}_{-2.4\%}$	$^{+23.2\%}_{-2.4\%}$	0.5%	0.5%
Background model of the fit	2.8%	1.3%	0.2%	0.2%
Trigger effects and reconstruction effects	1.1%	1.0%	1.2%	1.1%
B-meson lifetime uncertainty	1.0%	0.9%	< 0.1%	< 0.1%

Table 7: Summary of all systematic uncertainties for the number of signal events in the combined bin ($p_T > 13$ GeV, $|y| < 2.3$).

Source of uncertainty	Uncertainty value	
	$B_c^{\pm}$	$B^{\pm}$
Signal model of the fit	2.4%	0.1%
CS and PRD components	$^{+17.4\%}_{-2.4\%}$	0.5%
Background model of the fit	2.9%	0.1%
Trigger effects and reconstruction effects	0.9%	0.9%
B-meson lifetime uncertainty	0.7%	< 0.1%

pentaquak fit procedure

Fit to all kinematic distributions

- $M(J/\psi\ K\pi)$
- $M(J/\psi\ \pi K)$
- $M(J/\psi\ KK)$
- $M(J/\psi\ \pi\pi)$
- $M(J/\psi\ h)$ & $M(h_1h_2)$ in B^0 CR
- $M(J/\psi\ h)$ & $M(h_1h_2)$ in B_s CR

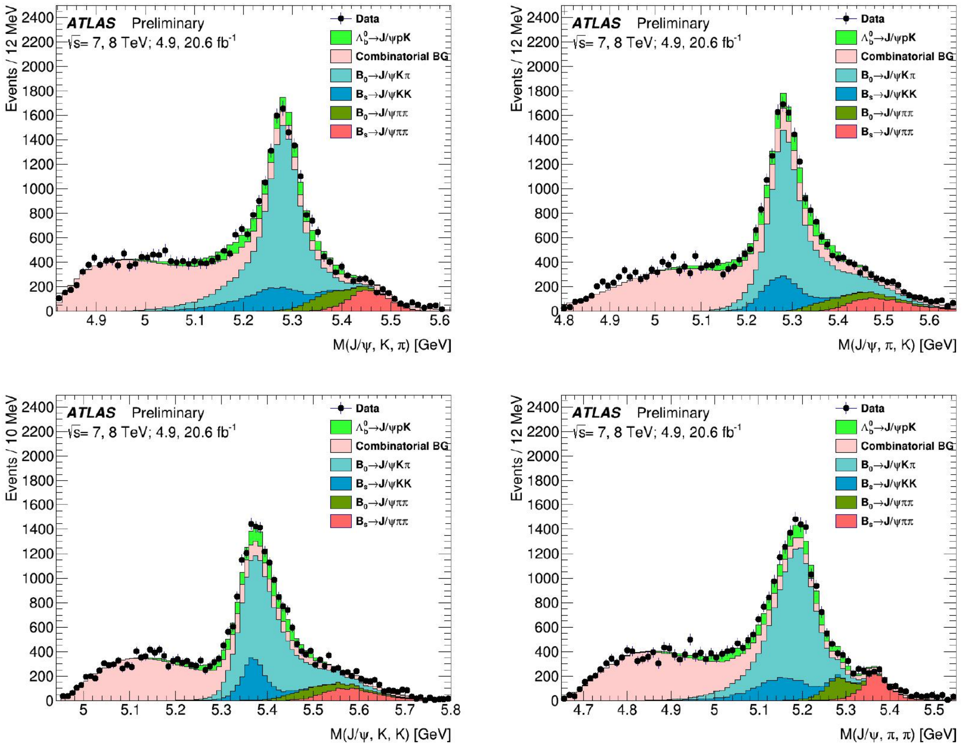

Figure 7: The $m(J/\psi, h_1 = K, h_2 = \pi)$, $m(J/\psi, h_1 = \pi, h_2 = K)$, $m(J/\psi, h_1 = K, h_2 = K)$ and $m(J/\psi, h_1 = \pi, h_2 = \pi)$ distributions for all selected H_b candidates. The "global" fit results are also shown.

pentaquak fit procedure

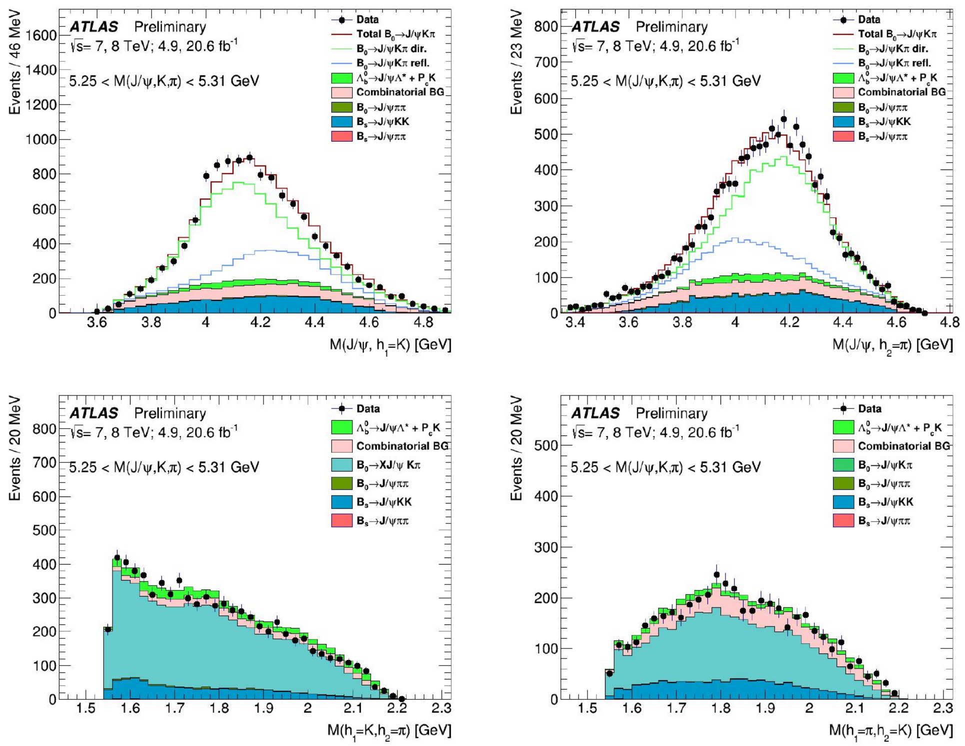

Figure 8: The $m(J/\psi, h_1 = K)$ (united with $m(J/\psi, h_2 = K)$), $m(J/\psi, h_2 = \pi)$ (united with $m(J/\psi, h_1 = \pi)$), $m(h_1 = K, h_2 = \pi)$ and $m(h_1 = \pi, h_2 = K)$ distributions for for events from the B^0 CR. The "global" fit results are also shown.

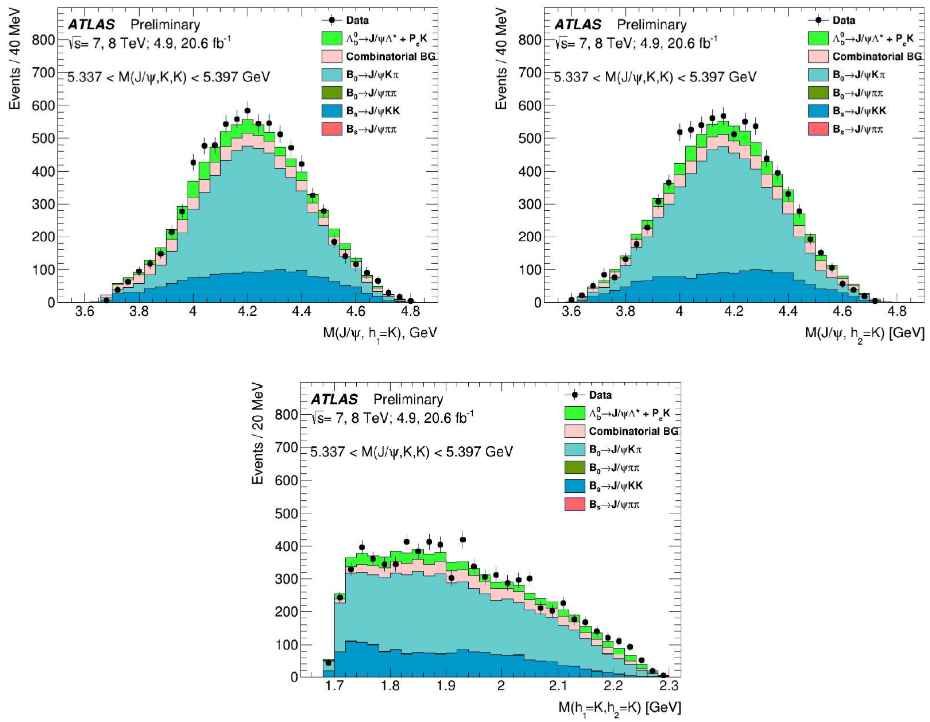

Figure 9: The $m(J/\psi, h_1 = K)$, $m(J/\psi, h_2 = K)$ and $m(h_1 = K, h_2 = K)$ distributions for for events from the B_s^0 CR. The "global" fit results are also shown.

pentaquak: uncertainty

Source	$N(P_{c1})$	$N(P_{c2})$	$N(P_{c1}+P_{c2})$	$\Delta\phi$
Number of $\Lambda_b^0 \to J/\psi p K^-$ decays	$^{+1.8}_{-0.6}\%$	$^{+6.6}_{-9.2}\%$	$^{+1.6}_{-0.8}\%$	$^{+0.3}_{-0.0}\%$
Pentaquark modelling	$^{+21}_{-0}\%$	$^{+1}_{-22}\%$	$^{+8.7}_{-4.4}\%$	$^{+1.6}_{-0.0}\%$
Non-pentaquark $\Lambda_b^0 \to J/\psi p K^-$ modelling	$^{+14}_{-2}\%$	$^{+5}_{-44}\%$	$^{+9.2}_{-9.1}\%$	$^{+3.6}_{-1.6}\%$
Combinatorial background	$^{+0.7}_{-4.0}\%$	$^{+18}_{-5}\%$	$^{+4.2}_{-4.8}\%$	$^{+3.2}_{-0.0}\%$
B meson decays modelling	$^{+13}_{-25}\%$	$^{+28}_{-35}\%$	$^{+1.6}_{-9.3}\%$	$^{+0.5}_{-2.1}\%$
Total systematic uncertainty	$^{+28}_{-25}\%$	$^{+35}_{-61}\%$	$^{+14}_{-15}\%$	$^{+5.1}_{-2.7}\%$

Table 2: Systematic uncertainties for measurements of the pentaquark yields under assumption of no interference effects, the yield of a sum of two pentaquarks and the relative phase between pentaquark amplitudes.

Source	$m(P_{c1})$	$\Gamma(P_{c1})$	$m(P_{c2})$	$\Gamma(P_{c2})$
Number of $\Lambda_b^0 \to J/\psi p K^-$ decays	$^{+0.06}_{-0.03}\%$	$^{+3.5}_{-2.5}\%$	$^{+0.07}_{-0.04}\%$	$^{+7}_{-13}\%$
Pentaquark modelling	$^{+0.6}_{-0.0}\%$	$^{+18}_{-0}\%$	$^{+0.2}_{-0.0}\%$	$^{+0}_{-33}\%$
Non-pentaquark $\Lambda_b^0 \to J/\psi p K^-$ modelling	$^{+0.23}_{-0.05}\%$	$^{+9.2}_{-1.2}\%$	$^{+0.24}_{-0.02}\%$	$^{+2}_{-62}\%$
Combinatorial background	$^{+0.03}_{-0.15}\%$	$^{+0}_{-11}\%$	$^{+0.01}_{-0.17}\%$	$^{+22}_{-4}\%$
B meson decays modelling	$^{+0.24}_{-0.00}\%$	$^{+21}_{-21}\%$	$^{+0.27}_{-0.14}\%$	$^{+17}_{-57}\%$
Total systematic uncertainty	$^{+0.7}_{-0.2}\%$	$^{+30}_{-24}\%$	$^{+0.4}_{-0.2}\%$	$^{+28}_{-91}\%$

Table 3: Systematic uncertainties for measurements of the pentaquark masses and natural widths.

The systematic uncertainties are summarised in Tables 2 and 3. Contributions from the systematic uncertainties listed above are added in quadrature separately for positive and negative variations.